J. Mex. Chem. Soc. **2024**, *68*(1)
Special Issue

ISSN-e 2594-0317

In Vitro and *In Silico* Studies of *Bis*-furyl-pyrrolo[3,4-*b*]pyridin-5-ones on Dengue Virus

Ivette Morales-Salazar[1], Carlos E. Garduño-Albino[1], Flora P. Montes-Enríquez[1], Atilano Gutiérrez-Carrillo[1], Yareli Rojas-Aguirre[2], Nancy Viridiana Estrada-Toledo[3], Jorge Sandoval-Basilio[4], Sofía Lizeth Alcaraz-Estrada[5*], Erik Díaz-Cervantes[6*], Eduardo González-Zamora[1*], Alejandro Islas-Jácome[1*]

[1]Departamento de Química, Universidad Autónoma Metropolitana-Iztapalapa, Av. Ferrocarril San Rafael Atlixco 186, Col. Leyes de Reforma 1A Sección, Iztapalapa, Ciudad de México, C.P. 09310, México.
[2]Departamento de Polímeros, Instituto de Investigaciones en Materiales, Universidad Nacional Autónoma de México, Circuito Exterior S/N, Ciudad Universitaria, Coyoacán, Ciudad de México, C.P. 04510, México.
[3]Coordinación de Comités de Evaluación en Salud, Centro de Investigación Clínica, Health Pharma Professional Research S.A. de C.V., Ciudad de México, C.P. 03100, México.
[4]Laboratorio de Biología Molecular, Universidad Hipócrates, Andrés de Urdaneta 360, Hornos, Acapulco de Juárez, Guerrero, C.P. 39355, México.
[5]División de Medicina Genómica, Centro Médico Nacional 20 de Noviembre, ISSSTE, Félix Cuevas 540, Col. Del Valle Sur, Benito Juárez, Ciudad de México, C.P. 03100, México.
[6]Departamento de Alimentos, Centro Interdisciplinario del Noreste, Universidad de Guanajuato, Tierra Blanca, Guanajuato, C.P. 37975, México.

***Corresponding author:** Sofía Lizeth Alcaraz-Estrada, email: sofializeth@gmail.com; Erik Díaz-Cervantes, email: e.diaz@ugto.mx; Eduardo González-Zamora, email: egz@xanum.uam.mx; Alejandro Islas-Jácome, email: aij@xanum.uam.mx

Received July 13th, 2023; Accepted November 17th, 2023.

DOI: http://dx.doi.org/10.29356/jmcs.v68i1.2103

Abstract. A series of six *bis*-furyl-pyrrolo[3,4-*b*]pyridin-5-ones synthesized *via* an Ugi-Zhu reaction coupled to a cascade process [*aza* Diels-Alder cycloaddition/*N*-acylation/aromatization] were evaluated *in vitro* against Dengue virus serotype 4 infection, and the Dengue virus replicon system encoding a *Renilla* luciferase gen reporter. Also, *in silico* studies on the non-structural protein 3 (NS3), a flavivirus protease comprising an attractive target for development of therapeutic antivirals bound to non-structural protein 2B (NS3-NS2B) were performed. The *in vitro* results showed that compounds **1a** and **1b** reduced the expression of *Renilla* luciferase in 44.2 and 31.6%, respectively. Additionally, the same compounds decreased viral load**,** thus revealing their potential activity against Dengue virus serotype 4. From *in silico* simulations, it was developed a NS3-NS2B model, which was used as a target for the studied molecules. Computational results agree with experimental data, showing that **1a** is the best ligand. Finally, a pharmacophoric model was computed for NS3-NS2B, which shows that the ligands need two hydrophobic and one hydrophilic fragment. Such results suggest that two out of the six synthesized *bis*-furyl-pyrrolo[3,4-*b*]pyridin-5-ones derivatives presents potential antiviral activity against Dengue virus *in vitro*.
Keywords: Dengue virus replicon; dengue virus serotype 4; *in vitro* assays; *in silico* simulations; docking; pyrrolo[3,4-*b*]pyridin-5-ones; Ugi-Zhu reaction.

Resumen. Una serie de seis *bis*-furil-pirrolo[3,4-*b*]piridin-5-onas sintetizadas *vía* una reacción Ugi-Zhu acoplada a un proceso en cascada [cicloadición *aza* Diels-Alder/*N*-acilación/aromatización] fueron evaluadas *in vitro* contra

J. Mex. Chem. Soc. **2024**, *68*(1)
Special Issue

ISSN-e 2594-0317

infección por el serotipo 4 del virus del dengue y el sistema de replicón del virus del Dengue que codifica un gen reportero de la luciferasa de la *Renilla*. Además, se realizaron estudios *in silico* sobre la proteína no estructural 3 (NS3), una proteasa de flavivirus que comprende un blanco atractivo para el desarrollo de antivirales terapéuticos unidos a la proteína no estructural 2B (NS3-NS2B). Los estudios *in vitro* revelaron que los compuestos **1a** y **1b** reducen la expresión de *Renilla* luciferasa en un 44.2 y 31.6%, respectivamente. Adicionalmente, estos compuestos redujeron la carga viral, revelando así su actividad potencial contra el virus del Dengue serotipo 4. Derivado de las simulaciones *in silico*, se obtuvo un modelo homólogo para NS3-NS2B, el cual fue considerado como blanco de las moléculas estudiadas. Los resultados computacionales correlacionan con los experimentales, mostrando que **1a** es el mejor ligando. Finalmente, se generó un modelo farmacofórico para NS3-NS2B, el cual muestra que los ligandos necesitan dos fragmentos hidrofóbicos y uno hidrofílico. Estos resultados demuestran que dos de los seis compuestos que se estudiaron presentan actividad antiviral *in vitro*.
Palabras clave: Replicón del virus del dengue; serotipo 4 del virus del dengue; ensayos *in vitro*; simulaciones *in silico*; docking; pirrolo[3,4-*b*]piridin-5-onas; reacción de Ugi-Zhu.

Introduction

Dengue virus (DENV) belongs to the genus Flavivirus and the family of *Flaviviridae* [1]. DENV comprises four serotypes, namely DENV1-4, that are genetically similar but antigenically distinct. However, all serotypes are infectious and pathogenic, and their circulation patterns fluctuate based on both geographical location and time [2]. DENV infection is a prevalent mosquito-borne disease occurring in tropical and subtropical regions. Globally, DENV infection cases range from 100 to 400 million and, 25,000 deaths [3], ranked second only for SARS-CoV-2, the causative agent of COVID-19 [4]. DENV infection manifests in various clinical conditions, including Dengue fever, Dengue hemorrhagic fever, and the highly dangerous Dengue shock syndrome [5,6]. In 2020, the vaccine Dengvaxia® (CYD-TDV) against DENV received approval. Developed by Sanofi-Pasteur, the vaccine aimed to alleviate the impact of DENV infection and its associated complications. As per the World Health Organization (WHO), Dengvaxia® demonstrated a reduction in morbidity of at least 25%, and its effectiveness and safety are influenced by previous exposure to the virus [7]. Given the suboptimal nature of current preventive measures and treatments for DENV, there is a genuine need to explore novel therapeutic alternatives to mitigate and potentially eradicate this disease.

Throughout the various stages of the DENV life cycle, several structural (S) and non-structural (NS) proteins play critical roles. The NS proteins found in DENV, including NS1, NS2A, NS2B, NS3, NS4A, NS4B, and NS5, are essential for viral genome replication, translation, viral polyprotein processing, encapsidation, and proper folding of viral proteins [2]. Among these NS proteins, those of utmost relevance due to their catalytic role are NS3, coupled with NS2B, as they are responsible for cleaving the polyprotein, a critical step in the DENV life cycle [8]. Consequently, NS3-NS2B emerges as an attractive target for the development of new drugs.

Subgenomic replicon systems are useful for identifying potential therapeutic molecules through efficient and high-throughput testing without extraneous and labor-intensive techniques [9,10]. In these systems, generally the genes that codify for the structural proteins of the virus are removed, preventing the generation of viral particles. Additionally, a reporter gene is inserted in the viral genome, enabling the monitoring of the replication process. The replicons follow the natural replicative cycle of the virus. Within the Flavivirus family, once inside the cell, the viral genome is translated into a polyprotein, which undergoes processing by cellular proteases and viral proteases. The proteolytic processing generates individual and functional viral proteins that facilitate the replication of the viral genome. Subsequently, copies of the viral genome initiate a new cycle [11] (Fig. 1). The interruption of any step of the cycle will be reflected in the reduction of the expression of the reporter gene. Replicons have been employed in the study of various Flaviviruses such as Yellow Fever [12,13], Hepatitis C Virus [14], West Nile [15,16], DENV [17,5] and Zika [18], including the assessment of the antiviral activity of a diversity of compounds, underscoring the value of these systems.

J. Mex. Chem. Soc. **2024**, *68*(1)
Special Issue

ISSN-e 2594-0317

In a previous work [19], we reported the synthesis of a series of six new *bis*-furyl-pyrrolo[3,4-*b*]pyridin-5-ones, which exhibited moderate activity against human SARS-CoV-2. By evaluating the efficacy of these compounds in the Dengue replicon system and DENV4 infection, we aim to investigate their potential as antiviral agents against DENV. This research carries significance as it offers an opportunity to explore the antiviral effectiveness of the initially investigated polyheterocycles against SARS-CoV-2. Understanding their effectiveness in inhibiting the replication of the DENV could provide valuable insights into the design of future therapeutics targeting this global health concern.

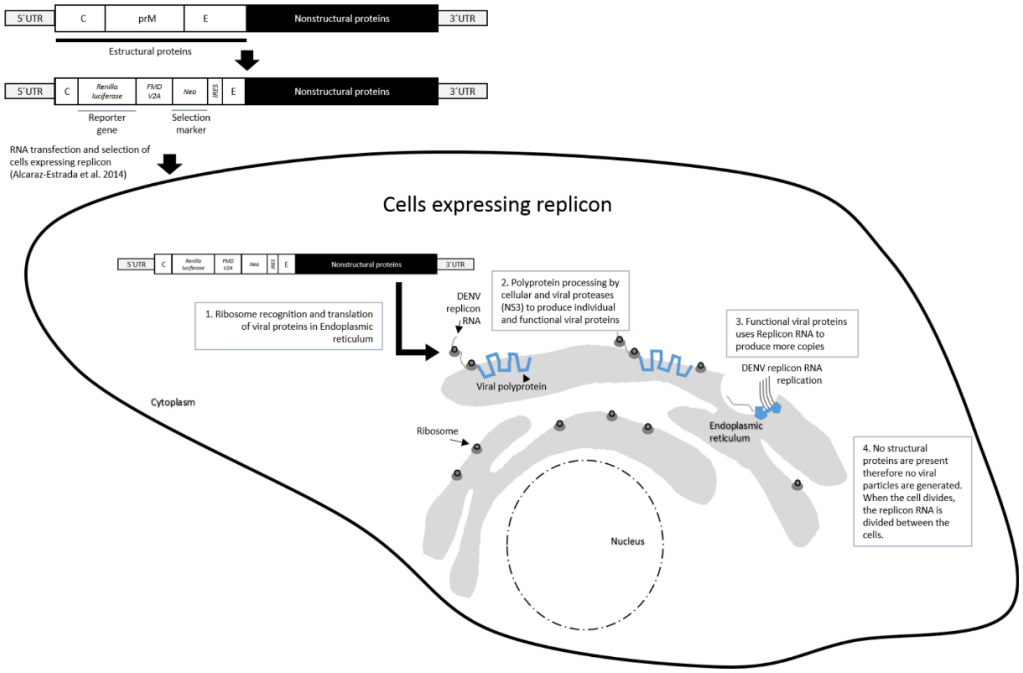

Fig. 1. Schematic representation of the replicon model. The DENV viral genome was modified to remove most of the structural viral proteins which were then replaced with the *Renilla* luciferase reporter gene and a selection gene. The RNA is transfected and once it reaches the cytoplasm, it is immediately recognized by ribosomes that generate the nascent viral polyprotein, which will be further processed by cellular proteases and by the viral protease (NS3) to produce individual and functional viral proteins. These proteins, in turn, will drive the replication of the viral genome.

Experimental

Materials

Synthesis

All starting reagents and solvents were used as received (without further purification, distillation, nor dehydration).

Cell line

Vero (African green monkey kidney) CCL-81 cells expressing DENV serotype 4 replicons were used [5]. Vero cells were cultured in Dulbecco's Modified Eagle's Medium high glucose (DMEM) (GibcoTM) supplemented with 10 % fetal bovine serum (FBS) (GibcoTM), glutamine 2 mM (Sigma-Aldrich-Merck) and G418 300 µg/mL (GibcoTM) and placed in 5 % CO_2 atmosphere at 37 °C.

J. Mex. Chem. Soc. **2024**, *68*(1)
Special Issue

ISSN-e 2594-0317

Instrumentation

Microwave-assisted reactions were performed in closed-vessel mode on a CEM Discover SP MW-reactor. Reaction progress was monitored by thin-layer chromatography (TLC) and the spots were visualized under ultraviolet (UV) light (254 or 365 nm). Flash columns packed with silica-gel 60, 230–400 mesh particle size and glass preparative plates (20 × 20 cm) coated with silica-gel 60 doped with UV indicator (F_{254}) were used to purify the products.

General method for the preparation of the assayed *bis*-furyl-pyrrolo[3,4-*b*]pyridin-5-ones 1a-f

The corresponding *bis*-furyl-pyrrolo[3,4-*b*]pyridin-5-ones **1a–f** were synthesized using the methodology reported by us [19]. Thus, in a sealed CEM Discover microwave reaction tube (10 mL) containing a stirring bar, corresponding aldehydes (1.00 equiv.) and amines (0.10 mmol, 1.00 equiv.) were diluted in dry toluene (1.00 mL). These mixtures were stirred and heated using microwave irradiation (65 °C, 100 W) for 5 minutes. Then, ytterbium(III) triflate (0.03 equiv.) was added and heated using microwave irradiation (65 °C, 100 W) for 5 minutes. The corresponding isocyanides (1.20 equiv.) were added and again heated using microwave irradiation (70 °C, 150 W) for 15 minutes. Finally, maleic anhydride (1.40 equiv.) was added, and the new reaction mixture was stirred and heated using microwave irradiation (80 °C, 150 W) for 15 minutes. At the end of the reaction time, the solvent was removed to dryness under vacuum. Then, extractions of the crude were carried out using dichloromethane (3 × 25 mL) to collect the organic phases, which were washed with brine (3 × 25 mL), dried in anhydrous Na_2SO_4, filtered, and concentrated to dryness. The new crude was purified by column chromatography using as stationary phase silica-gel followed by preparative TLC (20 x 20 cm) plates. The solvent mixtures of *n*-hexane (Hex) and ethyl acetate (EtOAc) in 1:1 or 1:2 (*v*/*v*) proportions were employed as mobile phase in both chromatography procedures to isolate the corresponding *bis*-furyl-pyrrolo[3,4-*b*]pyridin-5-ones **1a–f** in 45 to 82 % overall yields (Fig. 2).

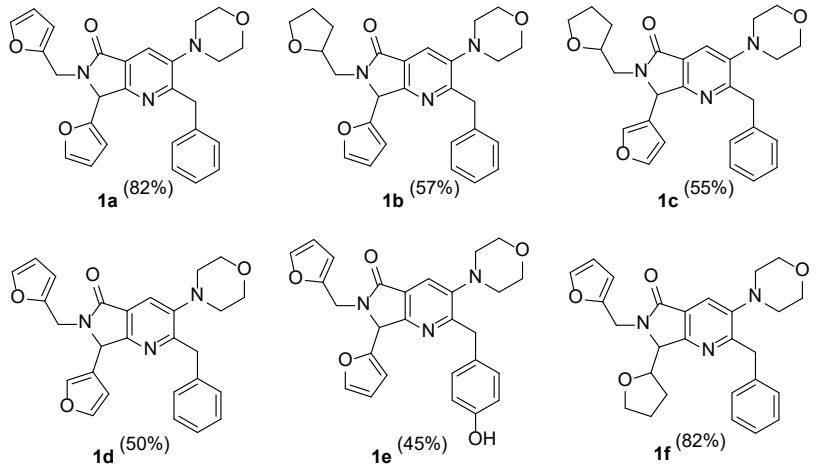

Fig. 2. Series of *bis*-furyl-pyrrolo[3,4-*b*]pyridin-5-ones **1a-f** synthesized via MCRs and *in vitro* assayed against DENV.

In vitro assays

Vero CCL-81 cell viability

The effect of the six *bis*-furyl-pyrrolo[3,4-*b*]pyridin-5-ones **1a–f** on Vero CCL-81 cell viability was determined as previously described [19]. Briefly, 24 h before the experiment 25000 cells/per well were placed in a 96-well plate using DMEM supplemented with 8% of FBS and glutamine in an incubator under 5% CO_2 atmosphere at 37 °C. The compounds were added at concentrations of 0.1, 1, 10, 100 μM in a final volume of

J. Mex. Chem. Soc. **2024**, *68*(1)
Special Issue

ISSN-e 2594-0317

100 µL of medium. After 48 h, media was removed and, 100 µL of crystal violet (0.1% crystal violet, 3.7% formaldehyde) were added. After 1 h at room temperature, plates were washed and 100 µL of 10% of acetic acid was added release to the dye. Plates were placed in an absorbance reader at a wavelength of 590 nm (Sunrise, TECAN) and cell viability was determined with respect to the vehicle control (DMSO). The experiments were performed three times in duplicates (n = 6). The vehicle refers to cells that were cultured in DMEM medium plus 0.5 % DMSO, which was the DMSO volume used in the diluent to solubilize the compounds.

Antiviral assay in DENV4 replicon system

The DENV4 replicon reporter assay was performed as previously described [5]. Briefly, 24 h before the assay, 25000 cell/per well of Vero cells were seeded in a 96-well plate. 10 µM of the compounds were added and after 48 h, the cells were lysed and *Renilla* luciferase was detected using *Renilla* Luciferase Assay System (Promega) and then measured using Luciferase reader (GloMax 20/20 Luminometer, Promega). Percent of expression was calculated normalizing the luciferase signal with the cells treated with vehicle (DMSO) (100 % of expression). Graph and statistical analysis were calculated using in GraphPad Prism version 9.5.1 (San Diego, CA, USA). p-Value was calculated using ordinary one-way-ANOVA test.

Antiviral assay Inhibition of DENV4 infection

For the infection inhibition assays of the Dengue virus serotype 2 and 4, 25000 Vero cells were seeded 24 h before infection. Infection was carried out at a multiplicity of infection (MOI) of 0.1 at 37 °C for 1 h. The addition of the compounds is as described above. Carnosine (L-CAR) was used as a positive control for replication inhibition since its direct interaction with the viral protein NS3-NS2B of DENV2 has been reported [20]. 24 h later, RNA was extracted from the collected supernatant using QuickExtract RNA Extraction Kit (Lucigen) following the supplier's recommendations. Briefly, the medium was removed from the cells, washed with 1x PBS, 50 µL cold Quick Extract RNA Extraction Solution was added, and the lysate was transferred to a 1.5 mL, vortexed for 1 min and heated for 2 min at 65 °C. Afterwards, 5.5 µL of DNase Buffer 1, 1.25 µL of RiboGuard RNase Inhibitor, 2.5 µL of RNasefree DNase were added and heated for 15 min at 37 °C. Finally, 2 µL of Stop Solution was added and incubated for 10 min at 65 °C. Subsequently, the RT-qPCR was carried out in CFX96 Touch Real Time PCR Detection System (Bio-Rad) using OneStep RT-PCR Kit (Qiagen) to determine viral load following the supplier's recommendations. Briefly, 10 µL of 5x QIAGEN OneStep RT-PCR Buffer, 2 µL of dNTP Mix, 0.6 µM of forward primer 5′-TTGAGTAAACYRTGCTGCCTGTAGCTC-3′ and 0.6 µM of reversed primer 5′-GAGACAGCAGGATCTCTGGTCTYTC-3′[21], 2 µL of OneStep RT-PCR Enzyme Mix, 50 µg of RNA and 1 µL of Eva Green (Biotium). The RT-qPCR conditions were 50 °C for 30 min and 95 °C for 15 min, followed by 40 cycles of 94 °C for 30 sec, 55 °C for 30 sec and 72°C for 30 sec. Fluorescence quantification was performed during the extension step. The viral load of the dengue virus was obtained with the -2^(ΔCT) method [22] and analyzed by two-way Anova in the Graph Pad V5 software using, p-values ≤0.05 w. The decrement of the viral load in each assay was compared to the vehicle, which was DMSO and was used as the negative control.

In silico studies

The *in silico* analyzes were carried out specifically on the protein used in the *in vitro* assays. A homology model of the DENV4 replicon has been computed using the Swiss-model server [23] and their sequence of amino acids, and so called NS3-t4. Also, it was considered the NS3-NS2B protein with their cofactor (NS2b) for the serotype-4 (PDB code: 2FOM, NS3/NS2B-t4). On the other hand, the *bis*-furyl-pyrrolo[3,4-*b*]pyridin-5-ones **1a-f**, as well as a control molecule (carnosine) [20] were modeled using the Avogadro package [24] and optimized through the generalized gradient approximation functional development by Perdew, Burke, and Erzerhof (PBE) [25] in the Gaussian 09 software [26].

The molecular docking was carried out using the Moldock [27] scoring function implemented in the Molegro Virtual Docker (MVD) package [28]. Finally, with ZincPharmer software [29] a pharmacophoric model was computed.

J. Mex. Chem. Soc. **2024**, *68*(1)
Special Issue

ISSN-e 2594-0317

Results and discussion

In vitro assays

The compounds under investigation were the six *bis*-furyl-pyrrolo[3,4-*b*]pyridin-5-ones **1a-f** that have previously shown moderate activity against the human SARS-CoV-2 [19]. By evaluating the efficacy of these compounds in the Dengue replicon system and using the viral particle, their potential as antiviral agents against DENV 4 were herein assessed.

The Vero cell line is considered as the standard model cell in dengue studies due to its infectability in response to dengue infection. This cell line is derived from African green monkey (*Chlorocebus sabaeus*) renal are classified into four major cell lineages: Vero JCRB0111, Vero CCL-81, Vero 76, and Vero E6. Each one of this cell lineages display specific features making them suitable for the propagation of certain viruses. For example, Vero CCL-81 is capable of propagating the Japanese encephalitis virus under prolonged culture conditions [12], West Nile Virus [30], Zika virus and DENV2 [31], while Vero E6 is used to propagate SARS-CoV-2 more efficiently [32]. The cell line expression in DENV replicon and infection used in this study was Vero CCL-81. As each subline has phenotypic and genetic differences [33]. It was relevant to determine the effect of the compounds on the Vero CCL-81 viability, despite their effect on Vero E6 viability was already investigated [19].

We observed a viability greater than 80% when Vero cells, expressing the DENV4 replicon, were exposed to the series of six compounds at the concentration of 10 μM (Fig. 3). At 100 μM, cell viability was reduced significantly, with the exception of compound **1f**. To note, these results align with the previous findings reported [19].

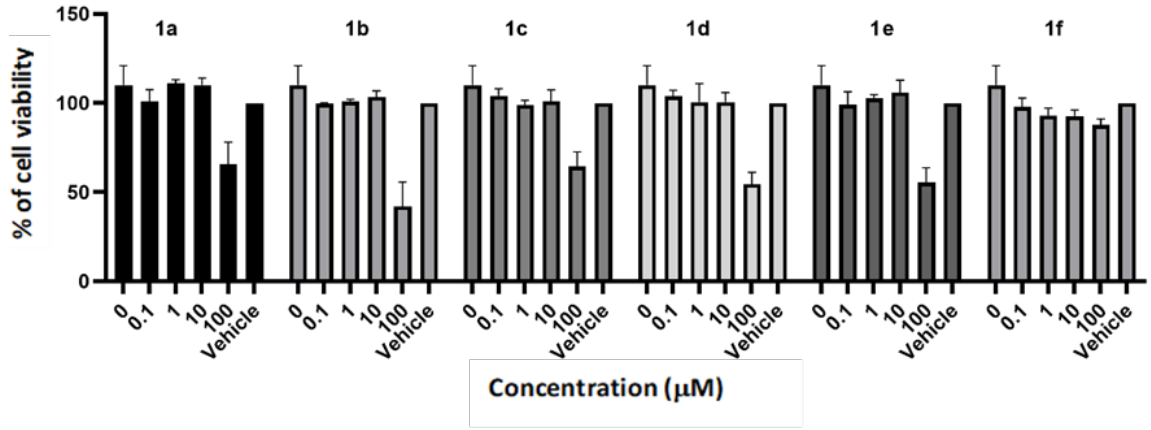

Fig. 3. Vero CCL-81 cell viability assays. The experiment was performed two independent times in triplicate and the bars depict the standard deviation of the mean (n = 6).

Antiviral activity on the Dengue virus replicon system

The antiviral activity on the DENV4 replicon of heterocyclic compounds was studied at 10 μM as this concentration did not affect the viability of Vero CCL-81 cells. Fig. 4 expresses the percentage of luciferase activity in y-axis that is a direct measurement of the viral genome translation and replication. Compounds **1c-f** did not reduce the expression of *Renilla* luciferase. On the other hand, compounds **1a** and **1b** showed a considerable reduction of the expression of the reporter gene, 44.2 % and 31.6 % respectively.

J. Mex. Chem. Soc. **2024**, *68*(1)
Special Issue

ISSN-e 2594-0317

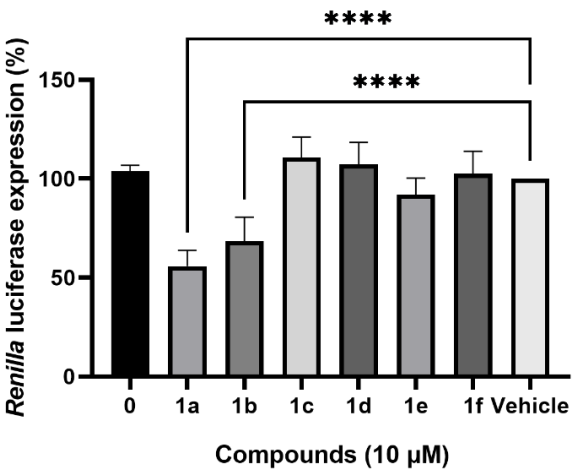

Fig. 4. Inhibition of DENV serotype 4 replicon replication and translation in Vero CCL-81 cells. The experiment was performed two independent times in triplicate and the bars depict the standard deviation of the mean (n = 6). **** p-Value = < 0.0001 using ordinary one-way-ANOVA test.

Antiviral activity on Dengue virus serotype 4

In this regard, DENV2 and DENV4 infection inhibition tests were carried out at 10 µM of the compounds (Fig. 5). In the case of DENV2, **1a** and **1b** did not reduced viral load, nevertheless with L-CAR we observed a reduction as reported (Figure S1 of Supplementary Materials File). The result obtained was that for DENV2 there is no reduction in viral load measured through RT-qPCR. Whereas that, **1a** y **1b** reduce in the viral load of DENV4 with respect to compounds **1c-1e**, L-CAR and negative control, although this trend was observed, it was not statistically significant (Fig 5).

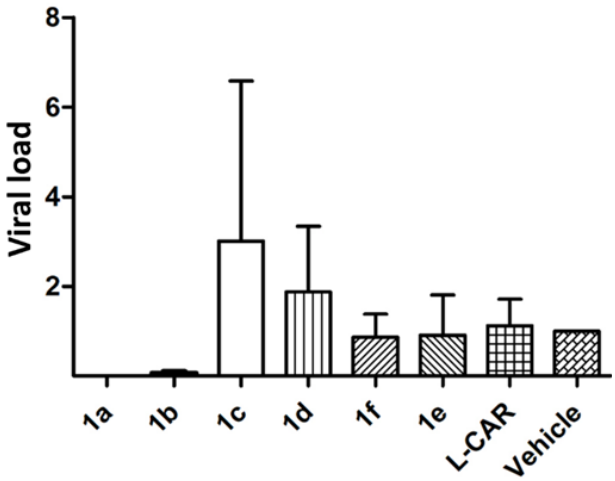

Fig. 5. Inhibition of DENV4 serotype 4 infection in Vero CCL-81 cells. The experiment was performed three independent times in duplicate and the bars depict the standard deviation of the mean (n = 6).

J. Mex. Chem. Soc. **2024**, *68*(1)
Special Issue

ISSN-e 2594-0317

The results indicate that compounds **1a** and **1b** have an antiviral effect in the replicon model and DENV4 infection. The specific inhibition observed in **1a** and **1b** could be due to the genome variability between serotypes and particularly for NS3, the conserved regions of the protein are few [34]. The same behaviorcan be observed for the positive control L-CAR that reduces the viral load specifically for DENV2 in our results but not DENV4.

As **1a** is the one with the highest activity, which may be due to interactions directed by the furane heterocycle in compound **1a**. Differences between compounds **1a** and **1b** are found in the furan and tetrahydrofuran heterocycles that decorates pyrrolo[3,4-*b*]pyridin-5-one core.

This result seems to be in contrast when the series were evaluated against SARS-CoV-2 [19], in which **1a** and **1b** did not affect the viral infection. We must take into account that there are structural differences between the two proteases, where the SARS-CoV-2 protease requires its dimeric form to be active, DENV protease requires a protein cofactor (NS2B) to be active. Hence, the active sites differ, and for this reason, we see a difference between the preference of compounds with inhibitory capacity according to the viral protease [35]. Compounds of a similar nature have been tested against other members of the *Flaviviridae* family *e.g.* Zika virus and have been shown to interact with and affect the viral protease NS3-NS2B of this flavivirus [36]. Therefore, performed an *in silico* study to delve into the possible interactions between **1a** and **1b** and the viral proteases mentioned above.

In silico studies

The first results regarding the docking studies are presented in Fig. 6, which demonstrates that the synthesized molecules are docked into the NS3 and NS3-NS2B DENV4 serotype.

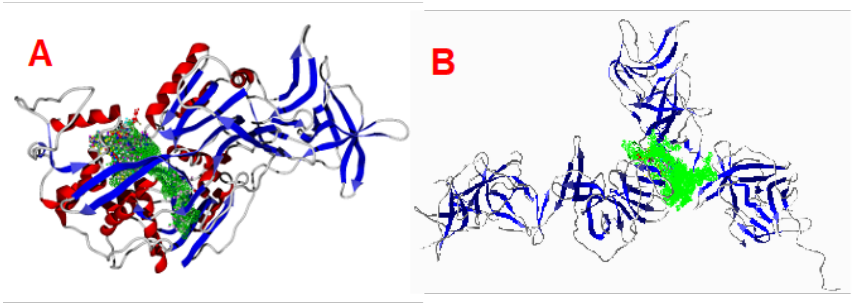

Fig. 6. Studied molecules docked into the **(A)** modeled NS3 DENV4 serotype-4 surface, **(B)** the NS3-NS2B DENV4 serotype-4.

Table 1. Ligand efficiency (LE) of the NS3-NS2B DENV4 serotype-4. All the values are in kcal/mol.

Molecule	LE	
	NS3-t4	NS3/NS2B-t4
1a	-4.95	-4.57
1b	-4.68	-4.36
1c	-4.84	-4.33
1d	-4.85	-4.57
1e	-4.90	-4.52
1f	-4.92	-4.30
Carnosine	-6.32	-6.39

J. Mex. Chem. Soc. **2024**, *68*(1)
Special Issue

ISSN-e 2594-0317

Analyzing the results of Table 1, the interactions between the selected ligands and the NS3-t4 and the NS3/NS2B-t4 correlated with the experimental results, considering that the best ligand is **1a**. In this order, the best interactions were between **1a** and NS3-t4, which present -4.95 kcal/mol, compared with the value of NS3/NS2B-t4, -4.57 kcal/mol. In this order, it was decided to analyze the interactions with NS3-t4 with the studied molecules.

The results agree with the experimental data, see Table 2, mainly considering the better interacting molecule **1a**. Highlight that these results were computed using the NS3 free protein, without the possible co-factor, proving that this is a possibility of interaction between **1a-f** compounds with the NS3, which interacts before coupling NS3 with the co-factor.

Table 2. Principal interacting energies between the studied molecules and the NS3 protein. All the values are in kcal/mol.

Ligand	LE	Hbond	Electro	VdW
1a	-4.95	-1.63	-0.67	9.44
1b	-4.68	-3.94	0.09	-37.15
1c	-4.84	-0.76	-1.67	-25.29
1d	-4.85	0.00	-1.30	-43.35
1e	-4.90	-4.05	-1.15	-51.50
1f	-4.92	-1.68	0.47	-47.30
Carnosine	-6.32	-6.70	-0.91	-20.93

*LE is the ligand efficiency (LE = Energy/# heavy atoms). Hbond is the hydrogen bond interaction. Electro is the electrostatic interactions, and VdW is the Van der Waals interactions.

Regarding the kind of interactions between **1a** and NS3-t4, Fig. 7 shows the key interactions. As well as Fig. 8 shows the interactions between NS3 protein and carnosine. Carnosine presents better interactions than **1a** because the last presents few steric interactions, see Fig. 7 and 8. At the same time, Carnosine presents more hydrogen bond interactions than **1a**.

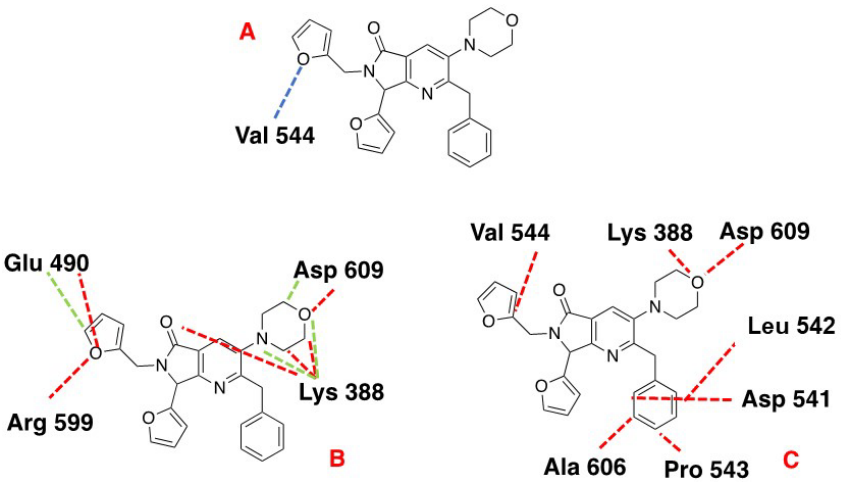

Fig. 7. (A) Hydrogen bond, **(B)** Electrostatic, and **(C)** Steric interactions between NS3 and **1a**. Blue lines depict the Hydrogen bond interactions, and Red and green dotted lines show the repulsive and attractive interaction, respectively.

J. Mex. Chem. Soc. **2024**, *68*(1)
Special Issue

ISSN-e 2594-0317

Fig. 8 shows that carnosine presents electrostatic interactions only with Lys 388, in contrast to **1a**, which presents electrostatic interactions with Asp 609, Arg599, and Glu490; see Fig. 6.

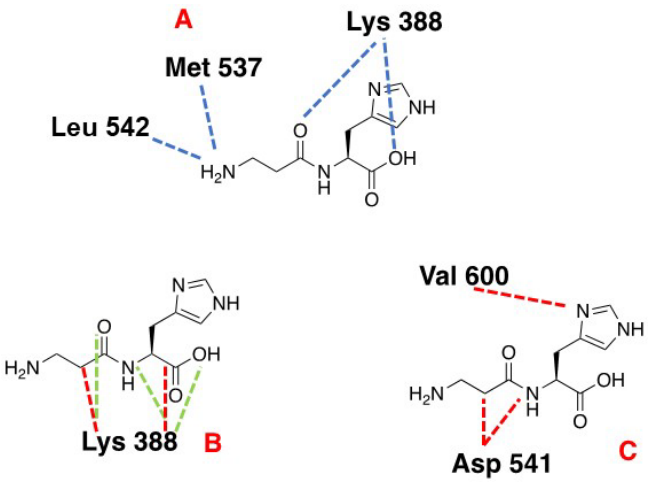

Fig. 8. (A) Hydrogen bond, **(B)** Electrostatic, and **(C)** Steric interactions between NS3 and carnosine. Blue lines depict the Hydrogen bond interactions, and Red and green dotted lines show the repulsive and attractive interaction, respectively.

In the case of hydrophobic interactions, the better-interacting cavity presents two hydrophobic surfaces surrounding a hydrophilic surface, see Fig. 9 **1a** presents interactions with both surfaces (hydrophobic) and, in the center, interacts with the hydrophilic surface (Fig. 9**(A)**). Carnosine only interacts with one hydrophobic surface and the hydrophilic surface in the center of the cavity, see Fig. 9**(B)**. The last can be the cause of finding a higher inhibitory effect with **1a** against serotype DENV4, which is more clearly shown in Fig. 9**(C)**, founding that carnosine, despite presenting a higher Ligand efficiency in the case of the hydrophobic interactions, needs some hydrophilic fragment to promote a better target-ligand interaction.

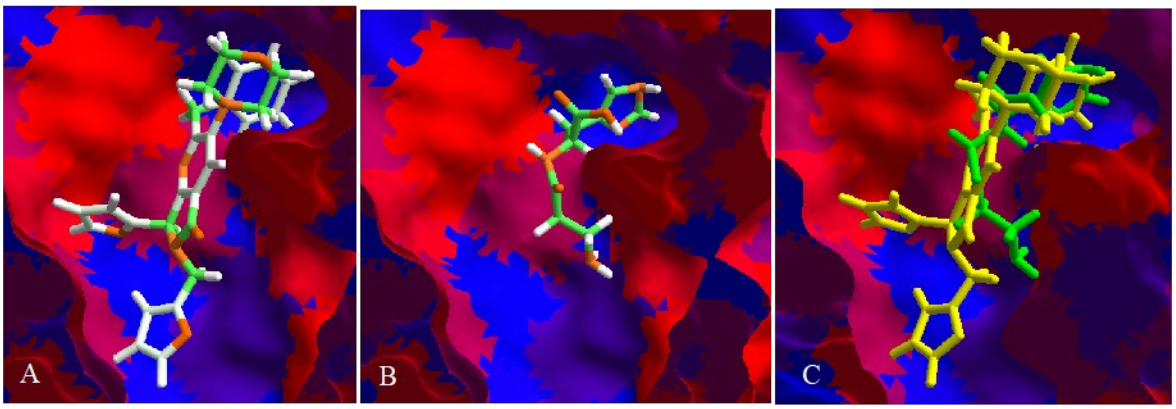

Fig. 9. Hydrophobic interactions between NS3 and A) **1a**, B) carnosine, and C) both molecules. Red surfaces show hydrophilic interactions and blue surfaces show hydrophobic interactions.

J. Mex. Chem. Soc. **2024**, *68*(1)
Special Issue

ISSN-e 2594-0317

Finally, a pharmacophoric model based on **1a** interactions was performed considering the whole ligand-receptor interactions. Fig. 10 shows that one molecule needs mainly six zones to better interact with NS3, these two hydrophobic-aromatic sites, other hydrophilic, and three hydrogen acceptor fragments. In agree with Fig. 9, one ligand proposed to link with NS3 needs only two hydrophobic fragments and one hydrophilic. Besides, Fig. 10 depicts carnosine and **1a** (Fig. 9**(B)**, and 10**(D)**, respectively) over pose into the pharmacophoric model, highlighting the need for two hydrophobic sites in the molecule to better interact with the NS3 target. Note that compounds that present higher LE and are not active can be due to the hydrophilic interactions and the need to modify their bioactive structure to interact with the pharmacophoric sites, such as the aromatic-hydrophobic site. Also, the bioactive pose is proposed around some factors, such as the whole functional groups of the molecule and the interactions of this with the target.

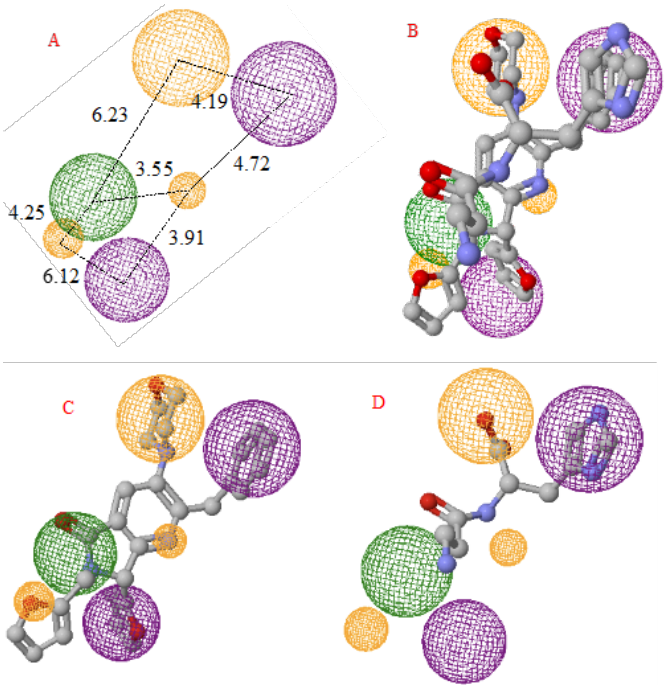

Fig. 10. **(A)** Pharmacophoric model for NS3 receptor **(B)** Pharmacophoric model with **1a**, and carnosine overlapping **(C) 1a**, and **(D)** Carnosine into the pharmacophoric model. The purple sphere depicts the hydrophobic-aromatic fragments, the orange sphere is the hydrogen acceptor fragments, and the green sphere is the hydrophilic fragments.

Conclusions

The results indicate that compounds **1a** and **1b** have an antiviral effect in the replicon model of DENV4 and DENV4 infection. The *in vitro* results showed that the compounds **1a** and **1b** exhibit antiviral effect (44.2 and 31.6 % respectively) in Vero cells that express DENV-4 virus.Commonly, replicon results are extrapolated to other DENV serotypes or even to other flaviviruses such as Zika. Interestingly, we show that the inhibition of compounds **1a** and **1b** are specific to DENV4, thus revealing their potential activity against DENV4.

An NS3 model was obtained *via* a homology model and used as a target for the studied molecules. Computational results agree with experimental data, which shows that the polyheterocycle **1a** is the best ligand. Finally, a pharmacophoric model was computed for NS3, which demonstrates that the ligands need two hydrophobic and one hydrophilic fragment.

J. Mex. Chem. Soc. **2024**, *68*(1)
Special Issue

ISSN-e 2594-0317

Acknowledgements

I.M.-S. thanks CONAHCYT – México for her PhD scholarship (947606). A.I.-J. acknowledges "Proyecto Apoyado por el Fondo Sectorial de Investigación para la Educación CONACyT-SEP CB-2017-2018 (A1-S-32582)" for financial support. E.D.-C. acknowledge to Dirección de Apoyo a Investigación y al Posgrado through the Convocatoria Institucional de Investigación Científica (CIIC) 2023, by the financed project 270/2023. Y.R-A acknowledges to PAPIIT-UNAM IA200821.

References

1. Alcaraz-Estrada, S. L.; Manzano, M. I. M.; Del Angel, R. M.; Levis, R.; Padmanabhan, R. *J. Gen. Virol.* **2010**, *91*, 2713–2718. DOI: https://doi.org/10.1099/vir.0.024083-0.
2. Yung, C. F.; Lee, K. S.; Thein, T. L.; Tan, L. K.; Gan, V. C.; Wong, J. G. X.; Lye, D. C.; Ng, L. C.; Leo, Y. S. *Am. J. Trop. Med. Hyg*. **2015**, *92*, 999–1005. DOI: https://doi.org/10.4269/ajtmh.14-0628.
3. Bhatt, S.; Gething, P. W.; Brady, O. J.; Messina, J. P.; Farlow, A. W.; Moyes, C. L.; Drake, J. M.; Brownstein, J. S.; Hoen, A. G.; Sankoh, O.; Myers, M. F.; George, D. B.; Jaenisch, T.; William Wint, G. R.; Simmons, C. P.; Scott, T. W.; Farrar, J. J.; Hay, S. I. *Nature.* **2013**, *496*, 504–507. DOI: https://doi.org/10.1038/nature12060.
4. Kok, B. H.; Lim, H. T.; Lim, C. P.; Lai, N. S.; Leow, C. Y.; Leow, C. H. *Virus Res.* **2022**, *324*, 199018. DOI: https://doi.org/10.1016/j.virusres.2022.199018.
5. Alcaraz-Estrada, S. L.; del Angel, R.; Padmanabhan, R., in: *Dengue. Methods in Molecular Biology*, Vol. 1138, Padmanabhan, R., Vasudevan, S., Eds., Humana Press, New York, NY, **2014**, 131–150. DOI: https://doi.org/10.1007/978-1-4939-0348-1.
6. Alcaraz-Estrada, S. L.; Yocupicio-Monroy, M.; Del Angel, R. M. *Future Virol.* **2010**, *5*, 575–592. DOI: https://doi.org/10.2217/FVL.10.49.
7. World Health Organization, https://www.who.int, accessed in June 2023.
8. Li, Z., Zhang, J.; Li, H. in *Viral proteases, and their inhibitors*, Gupta, S. P., Ed., Academic Press, **2017**,163–188. DOI: https://doi.org/10.1016/B978-0-12-809712-0.00007-1.
9. Hannemann, *H. Drug Discov. Today* **2020**, *25*, 1026-1033. DOI: 10.1016/j.drudis.2020.03.010.
10. Fernandes, R. S.; Freire, M. C. L. C.; Bueno, R. V.; Godoy, A. S.; Gil, L. H. V. G.; Oliva, G. *Viruses* **2020**, *12*, 598. DOI: https://doi.org/10.3390/v12060598.
11. Patil, V. M.; Balasubramanian, K.; Masand, N., in: *Dengue Virus Polymerase: A Crucial Target for Antiviral Drug Discovery*, Gupta, S. P., Ed., Academic Press, **2019**, 387–428. DOI: https://doi.org/10.1016/B978-0-12-815422-9.00014-0.
12. Saito, K.; Shimasaki, K.; Fukasawa, M.; Suzuki, R.; Okemoto-Nakamura, Y.; Katoh, K.; Takasaki, T.; Hanada, K. *Virus Res.* **2022**, *322*, 198935. DOI: https://doi.org/10.1016/j.virusres.2022.198935.
13. Jones, C. T.; Patkar, C. G.; Kuhn, R. J. *Virology.* **2005**, *331*, 247–259. DOI: https://doi.org/10.1016/j.virol.2004.10.034.
14. Satoh, S.; Mori, K.; Ueda, Y.; Sejima, H.; Dansako, H.; Ikeda, M.; Kato, N. *Plos one.* **2015**, *10*, e0118313. DOI: https://doi.org/10.1371/journal.pone.0118313.
15. Puig-Basagoiti, F.; Deas, T. S.; Ren, P.; Tilgner, M.; Ferguson, D. M.; Shi, P. Y. *Antimicrob. Agents Chemother*. **2005**, *49*, 4980–4988. DOI: https://doi.org/10.1128/aac.49.12.4980-4988.2005.
16. Alcaraz-Estrada, S. L.; Reichert, E. D.; Padmanabhan, R., In: A*ntiviral Methods and Protocols. Methods in Molecular Biology*, Vol. 1030, Gong, E. Eds., Humana Press, Totowa, NJ, **2013**, 283–299. DOI: https://doi.org/10.1007/978-1-62703-484-5_22.
17. Kato, F.; Hishiki, T. *Viruses.* **2016**, *8*, 122. DOI: 10.3390/v8050122.
18. Li, J. Q.; Deng, C. L.; Gu, D.; Li, X.; Shi, L.; Zhang, Q. Y.; Zhang, B.; Ye, H. Q. *Antivir. Res*. **2018**, *150*, 148–154. DOI: https://doi.org/10.1016/j.antiviral.2017.12.017.

J. Mex. Chem. Soc. **2024**, *68*(1)
Special Issue

ISSN-e 2594-0317

19. Morales-Salazar, I.; Montes-Enríquez, F. P.; Garduño-Albino, C. E.; García-Sánchez, M. A.; Ibarra, I. A.; Rojas-Aguirre, Y.; García-Hernández, M. E.; Sarmiento-Silva, R. E.; Alcaraz-Estrada, S. L.; Díaz-Cervantes, E.; González-Zamora, E.; Islas-Jácome, A. *RSC Med. Chem*. **2023**, *14*, 154–165. DOI: https://doi.org/10.1039/d2md00350c.
20. Rothan, H. A.; Abdulrahman, A. Y.; Khazali, A. S.; Nor Rashid, N.; Chong, T. T.; Yusof, R. *J. Pep. Sci*. **2019**, *25*, e3196. DOI: https://doi.org/10.1002/psc.3196.
21. García-Ruíz, D.; Martínez-Guzmán, M. A.; Cárdenas-Vargas, A.; Marino-Marmolejo, E.; Gutiérrez-Ortega, A.; González-Díaz, E.; Morfin-Otero, R.; Rodríguez-Noriega, E.; Pérez-Gómez, H.; Elizondo-Quiroga, D. *Springerplus.* **2016**, *5*, 1–9. DOI: https://doi.org/10.1186/s40064-016-2318-y.
22. Rao, X.; Huang, X.; Zhou, Z.; Lin, X. *Biostat. Bioinforma. Biomath*. **2013**, *3*, 71–85.
23. Waterhouse, A.; Bertoni, M.; Bienert, S.; Studer, G.; Tauriello, G.; Gumienny, R.; Heer, F. T.; de Beer, T. A. P.; Rempfer, C.; Bordoli, L.; Lepore, R.; Schwede, T. *Nucleic Acids Res*. **2018**, *46*, W296-W303. DOI: https://doi.org/10.1093/nar/gky427.
24. Hanwell, M. D.; Curtis, D. E.; Lonie, D. C.; Vandermeersch, T.; Zurek, E.; Hutchison, G. R. *J. Cheminform*. **2012**, *4*, 17. DOI: https://doi.org/10.1186/1758-2946-4-17.
25. Perdew, J. P.; Burke, K.; Ernzerhof, M. *Phys. Rev. Lett*. **1997**, *78*, 1396. DOI: https://doi.org/10.1103/PhysRevLett.77.3865.
26. Gaussian 09, Frisch, M. J.; Trucks, G. W.; Schlegel, H. B.; Scuseria, G. E.; Robb, M. A.; Cheeseman, J. R.; Scalmani, G.; Barone, V.; Mennucci, B.; Petersson, G. A.; Nakatsuji, H.; Caricato, M.; Li, X.; Hratchian, H. P.; Izmaylov, A. F.; Bloino, J.; Zheng, G.; Sonnenberg, J. L.; Hada, M.; Ehara, M.; Toyota, K.; Fukuda, R.; Hasegawa, J.; Ishida, M.; Nakajima, T.; Honda, Y.; Kitao, O.; Nakai, H.; Vreven, T.; Montgomery, J. A., Jr.; Peralta, J. E.; Ogliaro, F.; Bearpark, M.; Heyd, J. J.; Brothers, E.; Kudin, K. N.; Staroverov, V. N.; Kobayashi, R.; Normand, J.; Raghavachari, K.; Rendell, A.; Burant, J. C.; Iyengar, S. S.; Tomasi, J.; Cossi, M.; Rega, N.; Millam, J. M.; Klene, M.; Knox, J. E.; Cross, J. B.; Bakken, V.; Adamo, C.; Jaramillo, J.; Gomperts, R.; Stratmann, R. E.; Yazyev, O.; Austin, A. J.; Cammi, R.; Pomelli, C.; Ochterski, J. W.; Martin, R. L.; Morokuma, K.; Zakrzewski, V. G.; Voth, G. A.; Salvador, P.; Dannenberg, J. J.; Dapprich, S.; Daniels, A. D.; Farkas, Ö.; Foresman, J. B.; Ortiz, J. V.; Cioslowski, J.; Fox, D. J. Gaussian, Inc., Wallingford CT, **2009**.
27. Thomsen, R.; Christensen, M. H. *J. Med. Chem*. **2006**, *49*, 3315–3321. DOI: https://doi.org/10.1021/jm051197e.
28. Yang, J. M.; Chen, C. C. *Proteins* **2004**, *55*, 288–304. DOI: https://doi.org/10.1002/prot.20035.
29. Koes, D. R.; Camacho, C. J. *Nucleic Acids Res*. **2012**, *40*, W409–W414. DOI: https://doi.org/10.1093/nar/gks378.
30. McAuley, A. J.; Beasley, D. W. C. in: *West Nile Virus. Methods in Molecular Biology*, Vol. 1435, Colpitts, T., Ed., Humana Press, New York, **2016**, 19-27. DOI: https://doi.org/10.1007/978-1-4939-3670-0_3.
31. De Castro Barbosa, E.; Alves, T. M. A.; Kohlhoff, M.; Jangola, S. T. G.; Pires, D. E. V.; Figueiredo, A. C. C.; Alves, É. A. R.; Calzavara-Silva, C. E.; Sobral, M.; Kroon, E. G.; Rosa, L. H.; Zani C. L.; de Oliveira, J. G. *Virol. J*. **2022**, *19*, 31. DOI: https://doi.org/10.1186/s12985-022-01751-z.
32. Harcourt, J.; Tamin, A.; Lu, X.; Kamili, S.; Sakthivel, S. K.; Murray, J.; Queen, K.; Tao, Y.; Paden, C. R.; Zhang, J.; Li, Y.; Uehara, A.; Wang, H.; Goldsmith, C.; Bullock, H. A.; Wang, L.; Whitaker, B.; Lynch, B.; Gautam, R.; Schindewolf, C.; Lokugamage, K. G.; Scharton, D.; Plante, J. A.; Mirchandani, D.; Widen, S. G.; Narayanan, K.; Makino, S.; Ksiazek, T. G.; Plante, K. S.; Weaver, S. C.; Lindstrom, S.; Tong, S.; Menachery, V. D.; Thornburg, N. J. *Emerg. Infect. Dis*. **2020**, *26*, 1266. DOI: https://doi.org/10.3201/eid2606.200516.
33. Konishi, K.; Yamaji, T.; Sakuma, C.; Kasai, F.; Endo, T.; Kohara, A.; Hanada, K.; Osada, N. *Front. Genet*. **2022**, *13*, 801382. DOI: https://doi.org/10.3389/fgene.2022.801382.
34. Ayub, A.; Ashfaq, U. A.; Idrees, S.; Haque, A. *BioResearch Open Access.* **2013**, *2*, 392–396.
35. A) Lee, J.; Worrall, L. J.; Vuckovic, M.; Rosell, F. I.; Gentile, F.; Ton, A. T.; Caveney, N. A.; Ban, F.; Cherkasov, A.; Paetzel, M.; Strynadka, N. C. *Nat. Commun.* **2020**, *11*, 5877. DOI:

J. Mex. Chem. Soc. **2024**, *68*(1)
Special Issue

ISSN-e 2594-0317

https://doi.org/10.1038/s41467-020-19662-4. B) Lee, W. H. K.; Liu, W.; Fan, J. S.; Yang, D. *Biophys. J.* **2021**, *120*, 2444–2453. DOI: https://doi.org/10.1016/j.bpj.2021.04.015.

36. Soto-Acosta, R.; Jung, E.; Qiu, L.; Wilson, D. J.; Geraghty, R. J.; Chen, L. *Molecules.* **2021**, *26*, 3779. DOI: https://doi.org/10.3390/molecules26133779.